COBEM 2021 26th International Congress of Mechanical Engineering
November 22-26, 2021, Virtual Congress, Brazil

COB-2021-0439
VELOCITY MEASUREMENT OF LIQUID/GEL DROPLETS USING SHADOW IMAGES

Gabriel Silva Dias
Danilo Almeida Machado
Fernando de Souza Costa
Combustion and Propulsion Laboratory - LABCP
National Institute for Space Research - INPE
Rodovia Presidente Dutra, km 40, CEP 12.630-000
Cachoeira Paulista, São Paulo, Brazil
gabriel.dias@inpe.br

Abstract. *In this experimental work two identical impinging jet injectors were used to produce a fluid sheet. Two configurations were adopted, like and unlike impingement to form a liquid water/liquid water and a liquid water/gelled ethanol sheet, respectively. In order to compare those different configurations, the same jet momentum was adopted. The formed sheet undergoes fragmentation process. When the jet velocities are relatively low, droplets detach mainly from the rim's sheet and stays in the same plane, resulting essentially in a two-dimensional movement, differently from a completely developed spray, achieved with high jet velocities. An instrumented workbench with a high-speed camera and lenses were used to obtain shadow images of the atomization field. An open-source Particle Image Velocimetry (PIV) software was used to analyze batches of shadow images. The droplet and ligaments velocities presented a parabolic profile, in agreement with literature, demonstrating that shadow images together with open-source PIV is suitable for specific multiphase flows.*

Keywords: *droplet velocity, PIV, impinging jets, shadowgraph, atomization.*

1. INTRODUCTION

Impinging jet injectors are used in liquid rocket engines, as well as in some chemical processes. Such injectors are used when a rapid mixing between fluids is required, for instance, in rocket engines where a liquid fuel is mixed with the liquid oxidant to be subsequently burned. In order to improve mixing, a fuel jet collides with an oxidizer jet, resulting in rapid atomization and mixing. Experimental and theoretical studies on impinging jet atomization mechanisms (Ciezki and Ne, 2017), (Deng *et al.*, 2018), (Chen and Yang, 2019), (Ashgriz, 2011) show that when two jets with relatively low velocities (low u_j) collide at a certain impingement angle 2θ, they form initially a sheet in a perpendicular direction to the plane of the jets, then instabilities generate ligaments which are detached from the sheet at a certain breakup length, and eventually form drops as shown in Figure 1a.

Under typical flow conditions of liquid-propelled rocket engines, the sheet formed by impinging jets suffers a violent rupture caused by rapidly growing instability waves, commonly referred to as impact waves. Impact waves dominate the rupture and atomization processes by impinging jets (Chen and Yang, 2019).

The film, or sheet, (Figure 1b) is produced by a wide variety of injectors, including swirl and impinging jets injectors. When disintegration occurs through the movement of aerodynamic waves, a network of ligaments forms. Figure 1b indicates that waves grow on the leaf until they reach a critical amplitude. Ruptures at half the wavelength range occur in the ridges and valleys. The fragments contract into unstable ligaments due to surface tension, which later break into drops (Dombrowski and Johns, 1963)(Fakhri *et al.*, 2010).

Determining the velocity of a gaseous or liquid flow is not that easy, since they do not contain, in general, moving objects that reveal the velocity of the fluid. During the years, many measurement techniques have been developed to determine indirectly the flow velocity by measuring other quantities and then relate these quantities with velocity by physics relations, some examples are pressure (pressure probes), rotational speed (wind anemometer) and heat transfer (hot film, hot wire) (Raffel *et al.*, 2018). Digital Particle Velocimetry or simply Particle Image Velocimetry (PIV) is an optical qualitative and quantitative flow visualization technique, that allows placing sensors outside the flow region and to capture images of the whole flow field. One disadvantage is the high cost of the components required for a PIV system. An attractive alternative is the adoption of individual subsystems, instead of an entire PIV system. For that is needed basically a couple of images with a well know time step between then, and a software to compute data.

Two identical jet injectors are used to impinge two relatively low velocity jets of liquid water/liquid water and liquid

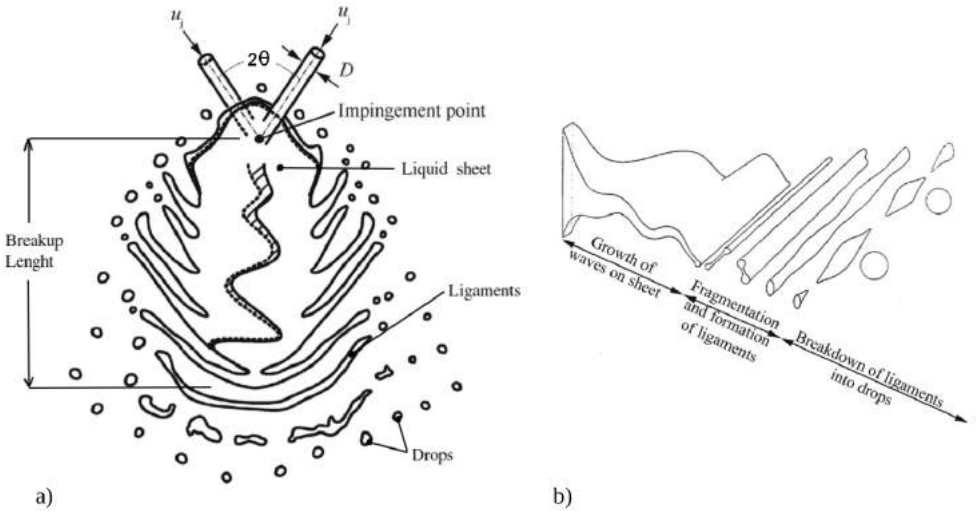

Figure 1. Two jet impinging scheme. Adapted from Chen and Yang (2019).

water/gelled ethanol. Velocity of droplets that detached from the sheet were recorded and a open-source PIV software were used to calculate their velocities. This work aims compare droplet velocity obtained from shadow images processed by an open source software with literature data.

2. METHODOLOGY AND MATERIALS

The materials used were liquid water and gelled hydrous ethanol. The gelled hydrous ethanol was characterized with an Anton Paar rheometer model MCR 72 at 25^oC according a power law fluid, yielding $\mu = 43.38\dot{\gamma}^{(0.20-1)}$ (K=43.38; n=0.20), where μ is the effective viscosity, K is the flow consistency index, $\dot{\gamma}$ is the shear rate and n is the flow behavior index.

This work used an instrumented workbench equipped with one liquid and one gel propellant tanks, inert gas cylinder, control valves, precision balance, timer, pressure data acquisition system besides a set-up of light, lens and a FASTEC TS3100SC4 high speed camera. The two identical inlet-chamfered jet injectors were made of Aluminium 6351 for atomization studies by impinging jets of liquids and gels. The injector had orifice diameter (*D*) of 0.8 mm and orifice length (*l*) of 8.0 mm, resulting in a ratio *l/D=10*.

Injection pressures versus ejected mass curves were built for the adopted pressure range considering the two working fluids. In order to compare results obtained for liquid water/liquid water to liquid water/gelled ethanol, the same jet momentum ($\dot{m}v$) were adopted during experimental impinging tests. When two jets of same jet momentum impinges, the sheet is formed in a plane that is parallel to the camera field of view plane, which is appropriated to two dimensions (2d) velocity measurements.

PIVlab software v2.30 was used to determine droplet velocities. It features a *multipass window deformation ensemble correlation*, which is especially helpful in micron-resolution particle image velocimetry (micro-PIV), as it can deal with very low seeding densities. This method requires to record a large number of images to obtain a more precise result (Stamhuis and Thielicke, 2014).

Figure 2 shows a screenshot of an important set-up on PIVlab, the interrogation area. In Digital PIV, the particle movement is calculated for groups of particles by evaluating the cross-correlation of many small sub images, called interrogation areas. The correlation yields the most probable displacement for a group of particles travelling on a straight line between two images (Stamhuis and Thielicke, 2014). When the areas overlap one another by, for example, 50% (step, Figure 2), there is additional displacement information at the borders and corners of each interrogation area. This information is used to calculate displacement information at every pixel of the interrogation areas via bi-linear interpolation (Stamhuis and Thielicke, 2014).

In order to get more accurate results, more passes (2 to 4 passes) are allowed. Their values do not need to be power of two as in Figure 2 (64, 32).

The peak finding technique is, as the cross correlation technique, an important factor for the accuracy of Digital PIV. The integer displacement of two interrogation areas can be determined directly from the location of the intensity peak of the correlation matrix. The location can be refined with sub-pixel precision using different procedures (Stamhuis and Thielicke, 2014). The standard procedure is to fit a Gaussian function to the integer intensity distribution. It is sufficient to use only the directly adjacent vertical and horizontal pixels (two times a 3-point fit = 2x3-point fit) and to evaluate the x and y axis individually (Stamhuis and Thielicke, 2014).

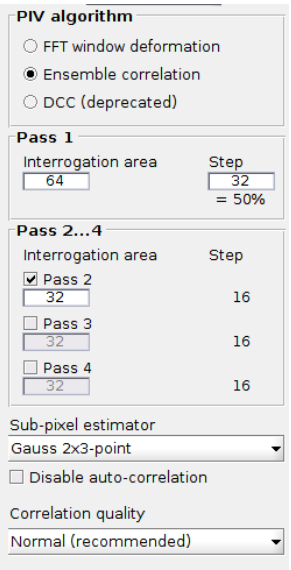

Figure 2. PIVlab ensemble correlation setup.

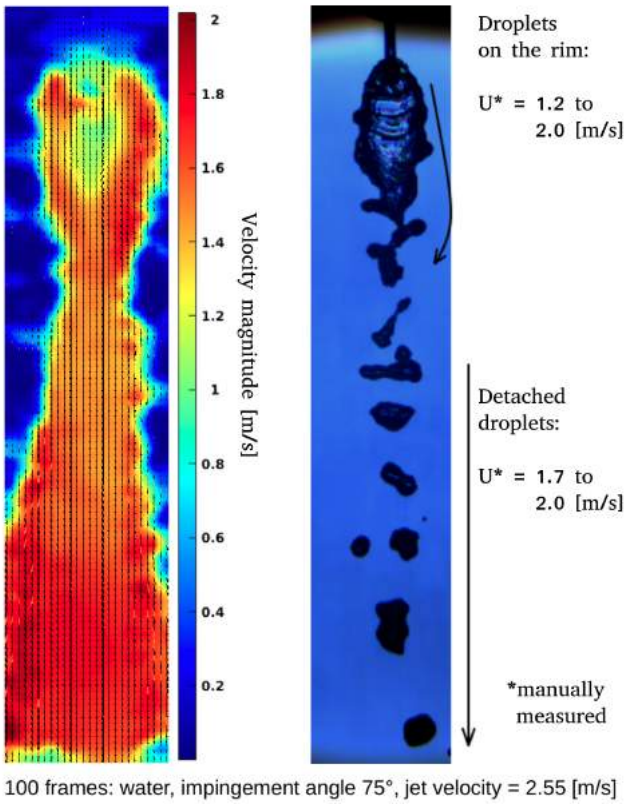

Figure 3. Velocity comparison - measured by hand vs PIVlab.

In this work, the shadowgraph images obtained with the high speed cameras with known time-steps were used to obtain the droplets velocities in specific cases. To calibrate the distance scale on PIVlab a picture of a caliper with 30 millimeters aperture was used.

In order to verify the method accuracy, velocities of six images in a row were calculated by hand from the changes in distances between recognizable droplets.

Figure 3 shows the manually calculated velocity magnitudes for 6 frames compared with the velocity field obtained by PIVlab for 100 frames. For manual calculations, detached particles were assumed to have only vertical movement while droplets on the rim had 2D movement. Droplets velocities on the rim were verified to have 1.5 m/s maximum values, such value were encountered by plotting velocities (magnitude) values over a line manually positioned in the rim. Detached droplets under the same procedure obtained a maximum value of 1.8 m/s. Taking the average value of manually measured velocities, the encountered error goes from 6.7% on the rim to 2.8% the detached droplets. It is interesting to note that not only droplets can be tracked by the PIVlab software, but also the instabilities on the sheet.

3. RESULTS

Before formation of a fully developed spray, the collision sheet stays inside a plane. If this plane is vertical and droplets detached remain in this plane, the Z component of the droplet velocity can be neglected. Considering this case, droplet velocities were determined from batches of shadow images with known shutter speed. About 300 to 400 images of liquid water like impingement and liquid water/gelled ethanol unlike impingement were processed using PIVlab ensemble correlation.

Jet conditions for experimental tests are in Table 1. The physical controled quantity was the injection pressure, so the jet momentum $(\dot{m}v)$ was calculated based on experimental Injection pressures versus ejected mass curves and considering the exit injector area.

Figure 4 shows a scatter plot and histogram for particle velocities during unlike impingement of gelled ethanol x liquid water, with jet momentum of 11 N and collision angle of 90^o.

As no mask were put to cover the sheet, the result represents ligaments and droplets. The u and v velocities represent horizontal and vertical velocities, respectively. Due to the impinging jet sheet and spray characteristics, the higher velocity is expected in the center-line. Although the scatter graph does not display distances, it is assumed that the region where $u = 0$ is the centerline. The denser red points region represents the most common velocity in the analysed area, including

Table 1. Jet velocities.

$\dot{m}$v [N]	Water Jet velocity [m/s]	Gelled Ethanol jet velocity [m/s]
6.40	3.57	4.01
6.50	3.60	-
9.66	4.39	-
11.00	4.69	5.20
31.00	7.86	8.66

the disintegrating sheet and droplets. The histogram shows the frequency of finding particle velocities as function of velocity magnitude $(u^2 + v^2)^{1/2}$. The greater the distance from the center-line, the lowest the v and the highest the u, drawing a parabolic profile. Similar profiles are found in literature Choo and Kang (2003), indicating that results with digital PIV with low cost lenses may be applied for particular cases.

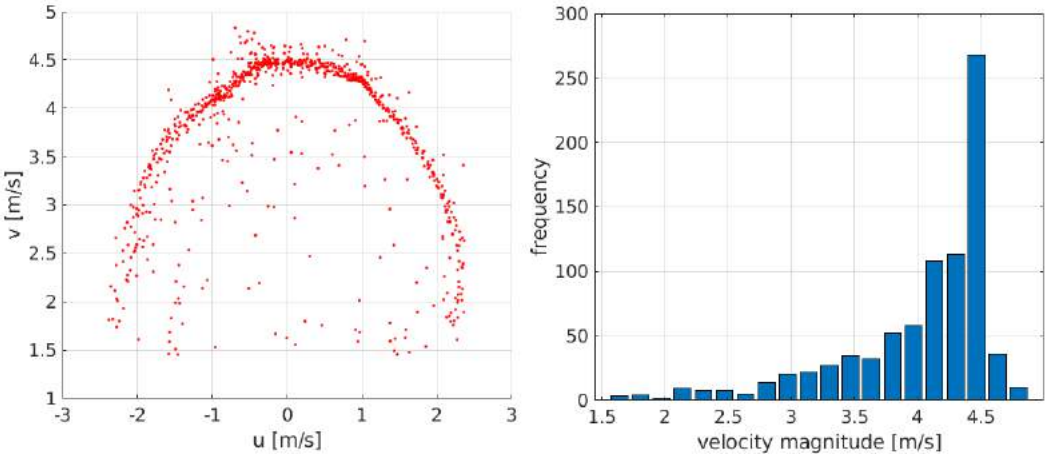

Figure 4. Particle velocities of ligaments and droplets for Unlike Impingement of Gelled Ethanol x Liquid Water, Jet momentum 11 N, $2\theta = 90^o$

In order to compare results for different collision angles in a single graph, the densest area of scattering was filled manually with points, as seen in Figure 5, and their coordinates were then plotted.

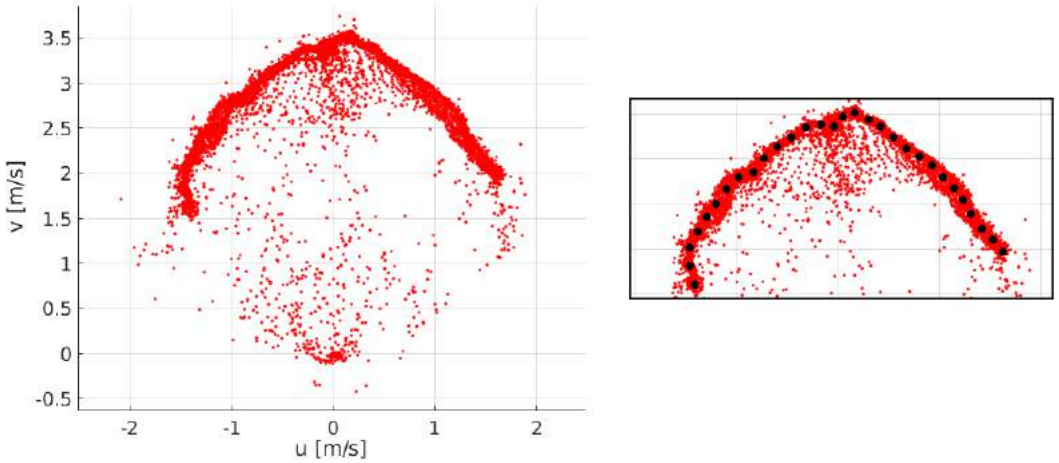

Figure 5. Densest area of scattering filled manually with points.

Figure 6 shows particle velocities for water like impingement with two different jet velocities and three different collision angles. The lower the collision angle, the highest the velocity on center-line, due to the vertical component momentum. The highest 2θ, the more spread the droplets become, so the approximately parabolic profile becomes elongated. Such intuitive results match the findings in Figure 6.

Choo and Kang (2003) reported similar results, as in Figure 7, where σ is the azimutal angle, V_L the ligament velocity and V_j is the jet velocity. In their work, they found values V_L/V_j from 0.88 to 0.89, as seen in Fig 7, with large standard

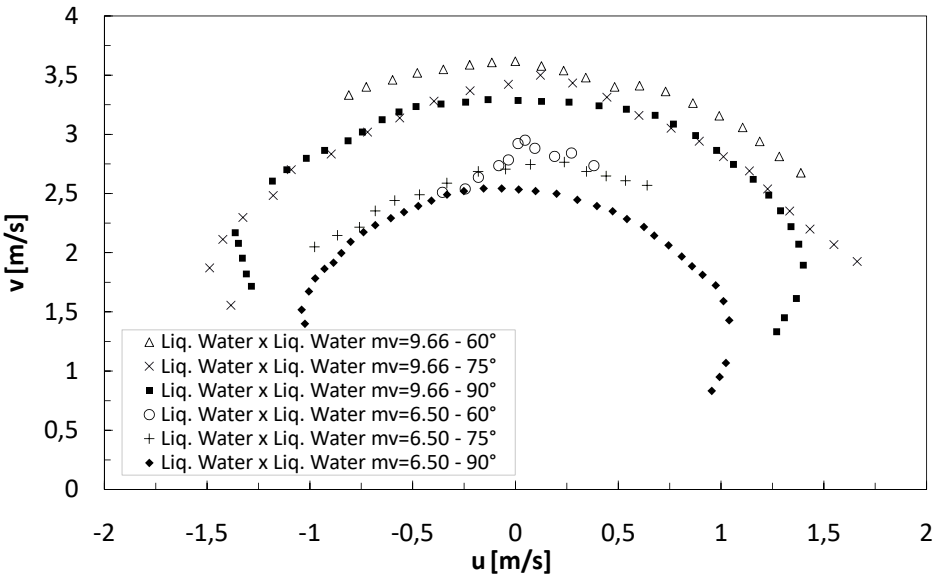

Figure 6. Particle velocities of ligaments and droplets for liquid water, like impingement

deviation, for $2\theta = 80^o$. The same ratio for the present work goes from 0.76 to 0.80 for $2\theta = 75^o$. Several factors may affect the ligament and droplet velocities, such as the jet pre-impingement velocity profile, that affects directly the sheet disintegration and subsequently the droplet and ligament velocities.

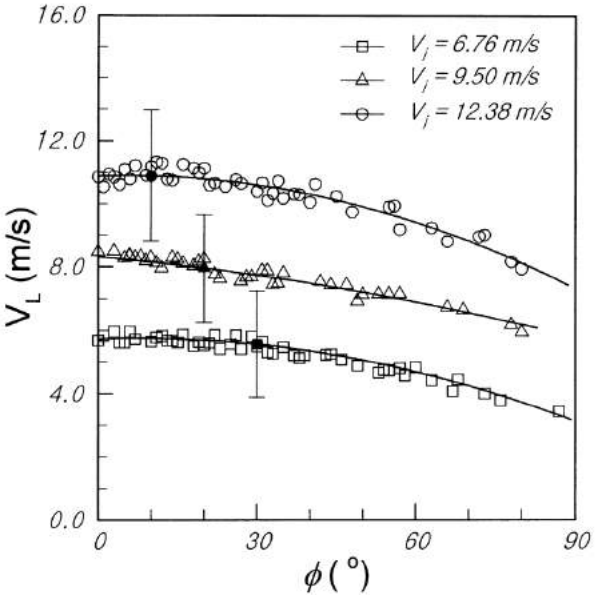

Figure 7. Ligament velocities varying jet velocity for $2\theta = 80^o$, from Choo and Kang (2003)

Figure 8 shows particle velocities for unlike impingement of gelled ethanol with liquid water and liquid ethanol. Similarly to previous results, approximately parabolic profiles in the scatter plot were found in most cases, with same trends with respect to 2θ and jet velocity. Droplet velocity/jet velocity ratio now increased due to the higher velocity of the gelled ethanol (Table 4.4), 0.87 to 0.98 and 1.00 for $2\theta = 75^o$, $\dot{m}v = 6.4$, 11 and 31 N, comparing to gel velocity jet. Although for jet momentum of 11 N there is a fully developed spray, with more droplets moving in the z direction, it was helpful to notice the increase in 2D Droplet velocity/jet velocity ratio.

Figure 9 depicts a side view analysis of the formed liquid/gel sheet. In that case a mask was put on the centerline, so the particles with velocity v_z are not the same as those ones with velocity v in Figure 8, those particles are a little apart center-line in z direction. The scatter graph reveals that the side with more droplets (left side, verified on shadow images) also reaches highest velocities. The u_z velocity reaches maximum values of 0.05 times the jet velocity.

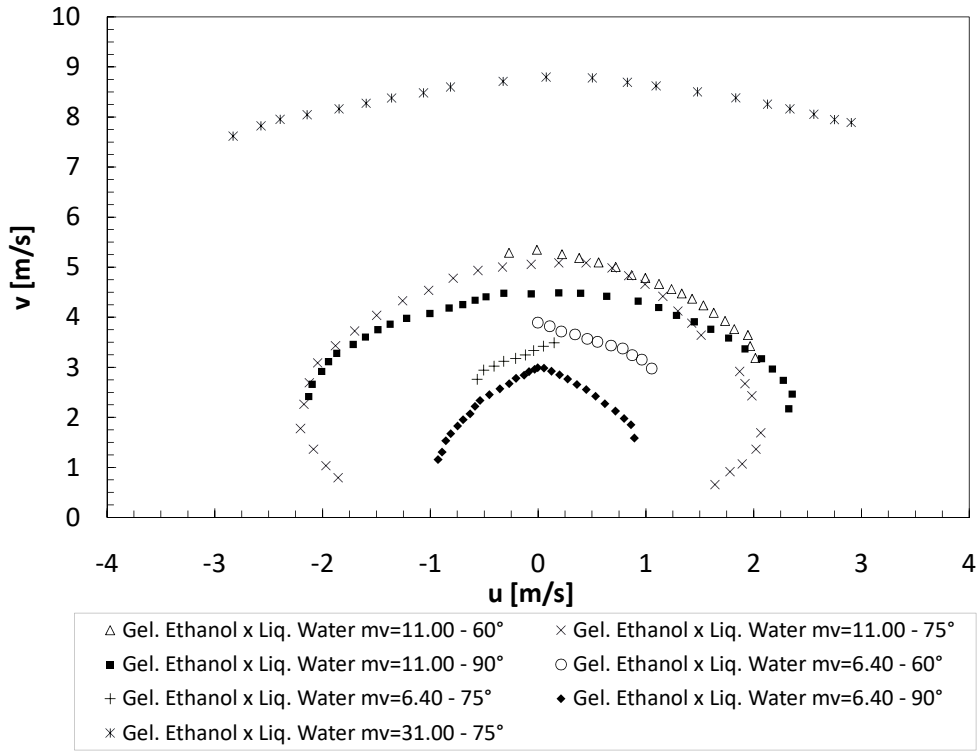

Figure 8. Particle velocities of ligaments and droplets for unlike impingement of gelled ethanol with liquid water.

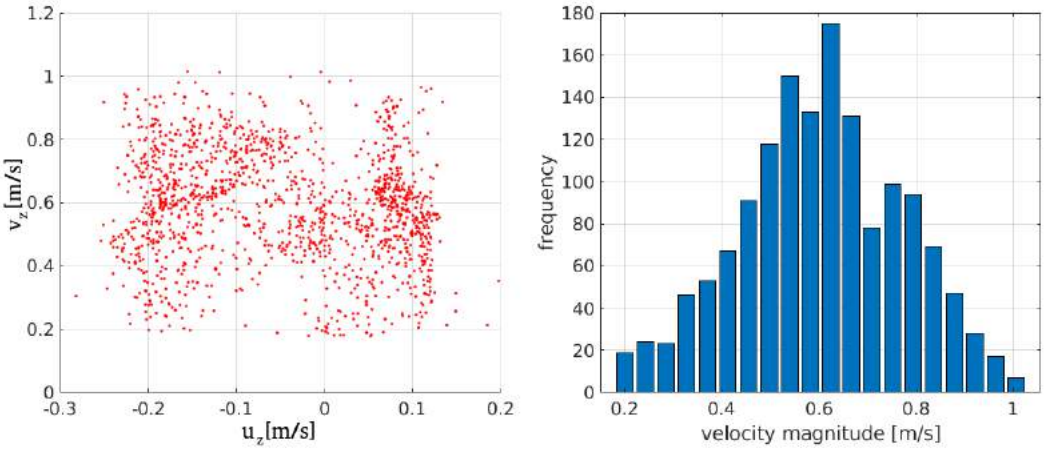

Figure 9. Droplet velocities for Unlike Impingement of Gelled Ethanol x Liquid Water, Jet momentum 11 N, $2\theta = 75^o$ - Scatter and histogram of particles in z direction

4. SUMMARY AND CONCLUSIONS

In this work shadow images of the collision sheets under know jet momentum were obtained with a high speed camera. An open Digital PIV software was used to calculate droplet velocities under specific conditions and showed good agreement with literature when batches of 300 to 400 images were processed. Detached droplets from the sheets formed a parabolic velocity profiles for liquid and liquid/gel configurations. Variations of impingement angle and jet momentum modified the velocity profile as expected. The z velocity component was analyzed for jet momentum equal to 11 N by taking side images of the liquid/gel sheet, maximum values of 5% of jet velocity were found.

5. ACKNOWLEDGEMENTS

The authors acknowledge FAPESP for support through process 2016/21957-0 and CAPES for the M.Sc. scholarship granted to the first author.

6. REFERENCES

Ashgriz, N., 2011. *Handbook of Atomization and Sprays*. Springer, New York.

Chen, X. and Yang, V., 2019. "Recent advances in physical understanding and quantitative prediction of impinging-jet dynamics and atomization". *Chinese Journal of Aeronautics*, Vol. 32, No. 1, pp. 45–57.

Choo, Y. and Kang, B., 2003. "A study on the velocity characteristics of the liquid elements produced by two impinging jets". *Experiments in Fluids*, Vol. 34, p. 655–661.

Ciezki, H. and Ne, 2017. "Atomization of viscoelastic fluids with an impinging jet injector: morphology and physical mechanism of thread formation". *Atomization and Sprays*, Vol. 27, pp. 319–336.

Deng, H., Feng, F. and Zhuo, C., 2018. "A simplified linear model and breakup characteristics of power-law sheet formed by a doublet impinging injector". *Proceedings of IMechE Part G: Journal Aerospace Engineering*, Vol. 232, pp. 1035–1046.

Dombrowski, N. and Johns, W., 1963. "The aerodynamic instability and disintegration of viscous liquid sheets". *Chemical Engineering Science,*, Vol. 18, pp. 203–214.

Fakhri, S., Lee, J. and Yetter, R., 2010. "Effect of nozzle geometry on the atomization and spray characteristics of gelled-propellant simultants formed by two impinging jets". *Atomization and Sprays*, Vol. 20, No. 12, pp. 1033–1046.

Raffel, M., Willert, C., Scarano, F., Kähler, C., Wereley, S. and KompenhansSettles, J., 2018. *Particle image velocimetry: a pratical guide*. Springer, Cham, Switzerland.

Stamhuis, E. and Thielicke, W., 2014. "Pivlab – towards user-friendly, affordable and accurate digital particle image velocimetry in matlab". *Journal of Open Research Software*, Vol. 2, No. 1.

7. RESPONSIBILITY NOTICE

The authors are the only responsible for the printed material included in this paper.